



RESEARCH LETTER

10.1029/2018GL080371

Key Points:

- Total rain volume (TRV) increases as aerosol optical depth (AOD) increases up to 0.4. TRV further decreases when AOD exceeds 0.5
- TRV change with AOD is strongest under favorable meteorological conditions (buoyancy, humidity, total precipitable water, and wind shear)
- The basic response of TRV to AOD is similar under all the meteorological conditions and during all stages of the MCS lifecycle

Supporting Information:

- Supporting Information S1
- Data Set S1
- Figure S1
- Figure S2
- Figure S3
- Figure S4
- Figure S5
- Figure S6
- Figure S7
- Figure S8

Correspondence to:

S. Chakraborty,
sudipm@ucla.edu

Citation:

Chakraborty, S., Fu, R., Rosenfeld, D., & Massie, S. T. (2018). The influence of aerosols and meteorological conditions on the total rain volume of the mesoscale convective systems over tropical continents. *Geophysical Research Letters*, 45, 13,099–13,106. <https://doi.org/10.1029/2018GL080371>

Received 11 SEP 2018

Accepted 5 NOV 2018

Accepted article online 9 NOV 2018

Published online 3 DEC 2018

The Influence of Aerosols and Meteorological Conditions on the Total Rain Volume of the Mesoscale Convective Systems Over Tropical Continents

Sudip Chakraborty¹ , Rong Fu¹ , Daniel Rosenfeld² , and Steven T. Massie³ 

¹Department of Atmospheric and Oceanic Sciences, University of California, Los Angeles, CA, USA, ²Institute of Earth Sciences, Hebrew University of Jerusalem, Jerusalem, Israel, ³Laboratory for Atmospheric and Space Physics, University of Colorado Boulder, Boulder, CO, USA

Abstract This study provides an observational assessment of the variations of the total rain volume (TRV) with aerosols through the entire lifetime of mesoscale convective systems (MCSs) over tropics. Using 70,000 MCSs' samples, we show that TRV increases with aerosols from clean to moderately heavy polluted conditions (aerosol optical depth [AOD] \sim 0.0–0.4). TRV decreases when AOD exceeds 0.5. The TRV change with AOD is strongest under favorable meteorological conditions, such as high total precipitable water (45–75 kg/m²), high convective available potential energy (1,200–2,400 J/kg), and intermediate vertical wind shear ($9\text{--}21 \times 10^{-4}$ /s). TRV of MCSs increases from 2 to 4 km³ (rain depth \sim 20–40 mm) when AOD < 0.15 or > 0.5, to more than 12 km³ (\sim 120 mm) when $0.2 < \text{AOD} < 0.4$ under above the mentioned optimal meteorological conditions. The basic response of TRV to aerosol concentrations is similar under all the meteorological conditions and during all stages of the MCS lifecycle.

Plain language summary Mesoscale convective systems (MCSs) contribute to the largest fraction of global rainfall and are often responsible for devastating flood events. It has long been hypothesized that aerosols can enhance rainfall of MCSs by suppressing rainfall during the early stage of the convection, enabling more cloud droplets to rise to higher altitude and so freeze. Freezing releases more latent heat, which drives strong rising motion and so enables formation of large hydrometeors for heavy rainfall. Thus, it is central to evaluate rainfall changes with aerosols through the entire lifetime of the MCSs. This work provides a first observational assessment of the variation of the total rain generated by MCSs through their lifetime with ambient aerosols, under various ambient meteorological conditions over the global tropical continents. Our results show that aerosols have a strong invigoration effect on MCSs' total rainfall volume. Total rainfall volume increases as AOD increases up to 0.4 and decreases as AOD increases beyond 0.5. Such effects are similar throughout different phases of their convective lifecycle and under various meteorological conditions.

1. Introduction

Mesoscale convective systems (MCSs), with radius of more than 100 kilometers, contribute to a large fraction of the total precipitation (Houze, 2004) and are the primary source of heavy precipitation over the tropics and midlatitudes (Schumacher et al., 2004), including floods (Houze et al., 2015). In addition to the influences from various meteorological parameters (Houze et al., 2015; Lee, 2012), studies in recent decades suggest that aerosols could also influence the intensity of MCSs (Fan et al., 2007; Lee, 2012; Lee et al., 2014; Stevens & Feingold, 2009; Tulet et al., 2010; Van Den Heever & Cotton, 2007) by either delaying or suppressing precipitation (Fan et al., 2013; D. Rosenfeld et al., 2007) and increasing the stratiform ice water content (de Boer et al., 2010; D. Rosenfeld & Lensky, 1998), anvil longevity (Tulet et al., 2010), and cloud top height (Bister & Kulmala, 2011). However, it is still unclear whether aerosols could influence the total volume of rainfall (TRV) produced during the entire lifetime of these MCSs. If so, how do these influences vary with meteorological conditions? Some studies show that aerosols enhance precipitation (A. Khain et al., 2005; A. P. Khain et al., 2008; I. Koren et al., 2010; van den Heever et al., 2006; Zhang et al., 2007), whereas other studies indicate that aerosols suppress rainfall (A. Khain et al., 2004; Lin et al., 2006; D. Rosenfeld, 1999, 2000) or that aerosols may not have any significant influence on the MCSs that produce heavy rainfall (Tao et al., 2012). While these variations of aerosol-rainfall relationships can be attributed to the differences in the meteorological conditions, convective types, aerosol types, limited samples of the convective systems, and measurements representing different

phases of convective lifetime also contribute to such variations. This study aims to address the latter two limitations, by the joint use of multiyear geostationary cloud data and polar satellite based precipitation radar data to determine aerosol-rainfall relationships for all stages of the convective life cycle for MCSs under various meteorological conditions over three tropical continents, including the Amazon, Congo, and Southeast Asia. In so doing, we will determine the changes of rainfall volume with aerosols through the life cycle of the MCSs under various meteorological conditions. To our knowledge, such evaluations have not been previously reported in literature.

Research in the literature has shown that the intensity of convection is influenced by total precipitable water (TPW; Holloway & Neelin, 2009), convective available potential energy (CAPE; Houze, 2004), vertical wind shear (VWS; Weisman & Rotunno, 2004), and lateral entrainment of free tropospheric humidity (relative humidity [RH]) as it contributes to a significant fraction of the total rainfall amount and parcel ascent (Langhans et al., 2015; Schumacher et al., 2004). Other studies suggest that aerosols' influence optimizes at aerosol optical depth (AOD) ~ 0.25 and increasing AOD beyond that value actually suppresses convection (Daniel Rosenfeld et al., 2008). The microphysical effect saturates at AOD ~ 0.3 , and beyond that value the impact of aerosols is reversed (Ilan Koren et al., 2008).

The physical mechanism behind the invigoration effect of aerosols on convection is that aerosols can delay precipitation, which allows more hydrometeors to glaciate. The latter releases more latent heating, consequently intensify rainfall during the mature and decay stages of the convection (Ilan Koren et al., 2008). Although intense convection/rainfall due to aerosol invigoration has been observed, it is unclear whether such instantaneous increase of rainfall would compensate the initial decrease of precipitation and lead to a statistically significant increase of the total rainfall during the lifetime of MCSs when large sample of MCSs across different tropical continents are considered. In addition, how meteorological parameters modulate the effect of aerosols on the total rainfall of MCSs is unknown. Aerosol-cloud effects are manifested throughout the cloud vertical dimension, and therefore, it is of interest to examine the effects of meteorology and aerosols upon the rainfall volume. In this study, we investigate the influences of aerosols on rainfall volume (TRV) during the growing, mature, and decay stages of the MCSs' lifecycle, under different meteorological conditions by analyzing more than 70,000 MCSs over three different tropical continents and for multi-year period (see section 2.2 and the supporting information). TRV considers the surface rain rate, longevity, and the area under MCSs at each stage of their convective lifecycle and represents the total rainfall produced by MCSs. We use TRV for this study because the volume of water (km^3) is more commonly used to describe extreme rainfall events and practical purposes such as water reservoir construction.

2. Data and Methods

2.1. Data Sets

We use the International Satellite Cloud Climatology Project (ISCCP) DX convection tracking and ISCCP B3 data sets to obtain information on the mesoscale systems at 3-hr intervals (Machado et al., 1998). We use TPW, RH, specific humidity, temperature, zonal wind, and geopotential height from the Modern Era Retrospective-Analysis for Research and Applications (MERRA; Rienecker et al., 2011), and rain rate from the TRMM 3B42 and 2A25 data sets. AOD information is taken from Aqua Moderate Resolution Imaging Spectroradiometer (MODIS) and MERRAero data sets. For details of the data sets used, please see the supporting information.

2.2. Methods

A total of 71,184 samples of MCSs representing different stages of convective lifecycle are obtained between January 2003 and June 2008 over equatorial Africa (10°N – 10°S , 10°W – 40°E), equatorial South America (5°N – 15°S , 40°W – 80°W), and South Asia (0 – 40°N , 70 – 100°E). For the South Asian region, we only analyze the monsoon months (June–August) of every year. We have used a domain of 2° latitude/longitude outside the periphery of MCSs to estimate ambient AOD, TPW, RH_{850} , and RH_{500} surrounding MCSs. CAPE, TRV, and VWS are calculated within the areas of MCSs. Satellite measurements of aerosols in the vicinity of clouds pose a large uncertainty due to the changes in RH, scavenging, and the 3-D radiative transfer (Remer et al., 2005; Tackett & Di Girolamo, 2009). In order to avoid erroneous values of AOD near convection (Varnai & Marshak,

2009), we only consider AOD from outside of a 2° radial distance from the boundary of the clouds (see supporting information S1).

TRV is calculated using the Tropical Rainfall Measuring Mission (TRMM), whereas the stages of lifecycle are determined using the ISCCP data sets. First, TRV for each phase of the convective life cycle is computed using the rainrate provided by TRMM 3B42 (Huffman et al., 2007; see the supporting information; an example is given in Figure S6). TRV of a MCS during the entire lifetime is estimated by integrating rainfall from all stages of the convective lifetime of that MCS. The corresponding values of TPW and AOD are averaged over the three different stages (see the supporting information). We then bin TRVs as a function of AOD and various meteorological parameters at three different stages of their convective lifecycle. We use increments of 15 kg/m^2 for TPW, 20% for RH, 600 J/kg for CAPE, and $3 \times 10^{-4}/\text{s}$ for VWS, respectively. For AOD, we have binned the data with an increment of 0.02 for AOD between 0.0 and 0.5. Then we have binned the data at an increment of 0.2 for AOD above 0.5. This is because the majority of the MCS lifecycle stages ($\sim 55,000$) are associated with AOD values less than 0.5 (Figure S3 in the supporting information). Figure S5 shows the standard errors in TRV in each bin as a function of TPW and AOD. The TRV of the MCSs for a given meteorological and AOD condition (bin) is calculated as the sum of the TRV for the growing, mature, and decay phases of the MCSs for the bin representing that meteorological and AOD condition. Thus, TRV only represents the statistical distribution of the total rainfall generated through the lifetime of all the MCSs in that bin and does not represent the total rainfall of each individual MCS.

3. Results

Figure 1 shows the average TRV obtained from all MCSs under various TPW and AOD values during each stage of the convective lifecycle (Figures 1b–1d) and also over the entire convective lifetime (Figure 1a). Figure 1 shows that TRV increases with TPW and is highest when TPW reaches $45\text{--}75 \text{ kg/m}^2$ (Figures 1a–1d), consistent with previous studies (Holloway & Neelin, 2009). Bins with mean TRV significantly different (p value = 0.05; see Figure S5) than two standard deviation (estimated by calculating Z scores) are shown. Under similar values of precipitable water, TRV during the entire MCSs' lifetime increases from less than 2 km^3 (RD or rain depth if the rainfall was evenly spread over the areas of the MCSs $\sim 20\text{--}30 \text{ mm}$) under very low AOD values (<0.1) to above 12 km^3 when AOD values range between 0.2 and 0.4 (Figure 1a). Amounts of RD corresponding to these large TRV values can accumulate to $120\text{--}150 \text{ mm}$. The range of RD depends on the size of the MCSs and varies with the amount of TPW they are associated with. TRV decreases to $3\text{--}8 \text{ km}^3$ ($40\text{--}80 \text{ mm}$) when AOD increases beyond 0.5 (Figure 1a). These variations in TRV are consistent during all three stages of the convective lifecycle (Figures 1b–1d) and over the entire lifetime (Figure 1a). During the growing and mature stages (Figures 1b and 1c), TRV increases from 1 to 1.5 km^3 when AOD is less than 0.2 or more than 0.5 to as much as 6 km^3 when AOD values are 0.2–0.5. Such increases in RD correspond to $10\text{--}30 \text{ mm}$ to $60\text{--}80 \text{ mm}$ and $5\text{--}20 \text{ mm}$ to $50\text{--}60 \text{ mm}$ when AOD and TPW conditions are optimal for the growing and mature stages, respectively. During the decaying stage, TRV (RD) increases from (1 km^3) $5\text{--}20 \text{ mm}$ to ($4\text{--}6 \text{ km}^3$) $30\text{--}50 \text{ mm}$ inside those optimal ranges, less than the other two stages.

Figure 2 shows the variation of TRV with AOD under various CAPE conditions. TRV increases with CAPE, which is consistent with previous findings (Houze, 2004). TRV increases as AOD increases, especially when CAPE is greater than $1,200 \text{ J/kg}$ (Figure 2a). Maximum values of TRV throughout the entire MCSs' lifetime are above 10 km^3 (Figure 2a) and occur within an optimal range of CAPE ($1,200\text{--}2,400 \text{ J/kg}$) and AOD (0.2–0.4). TRV also increases from 2.5 km^3 when CAPE is less than 600 J/kg and $\text{AOD} < 0.2$ or $\text{AOD} > 0.5$ to $3.5\text{--}8 \text{ km}^3$ when CAPE ranges from 600 to $2,400 \text{ J/kg}$ and $0.2 < \text{AOD} < 0.5$ during the growing and mature stages (Figures 2b and 2c). During the decaying stage (Figure 2d), TRV is generally lower and only reaches $3\text{--}6 \text{ km}^3$ when $\text{CAPE} > 1200 \text{ J/kg}$ and $0.2 < \text{AOD} < 0.4$. When AOD surrounding MCSs is greater than 0.4, TRV decreases during the entire lifetime (Figure 2a) and all three stages of the convective lifecycle (Figures 2b–2d).

VWS influences the dynamic organization and entrainment of the MCSs. Thus, we evaluate how the TRV-AOD relationship varies under different VWS in Figure 3. Consistent with that reported in the literature (Cotton & Anthes, 1989; Maddox et al., 1979), TRV increases from low to moderate ($3\text{--}21 \times 10^{-4}/\text{s}$) VWS (Figure 3a) and decreases under strong VWS ($>21 \times 10^{-4}/\text{s}$). However, the variations of TRV with AOD show a similar pattern as those in Figures 1 and 2. For a similar VWS condition, TRV increases with AOD when the AOD values are below 0.4 and decreases when AOD increases beyond 0.4 (Figures 3a–3d). TRV maximizes at AOD values

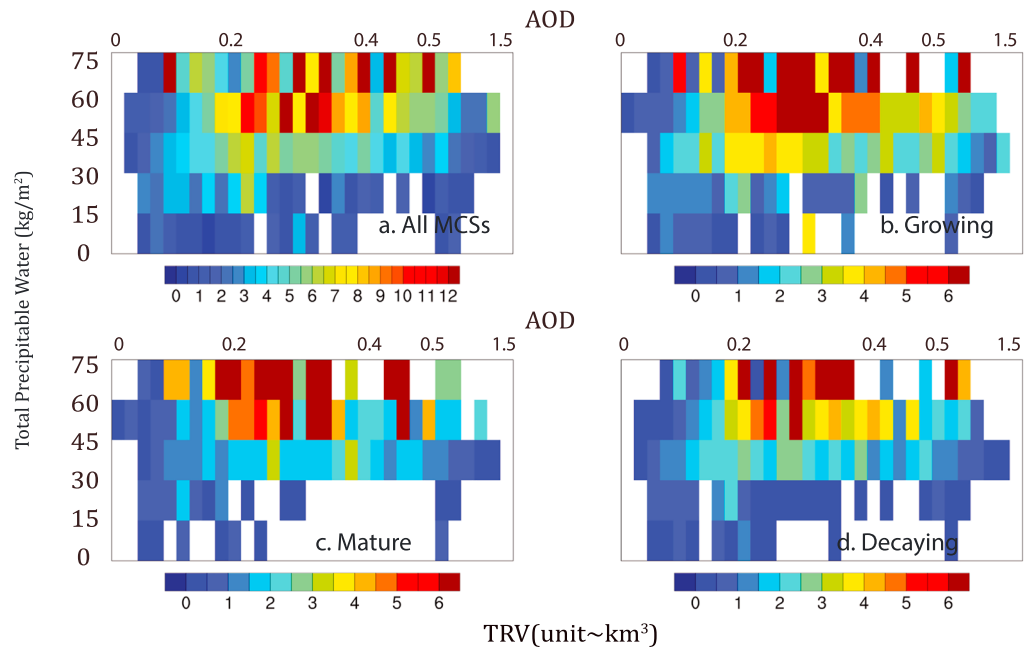


Figure 1. Total rain volume (TRV) under mesoscale convective systems as a function of TPW and aerosol optical depth (AOD) during (a) entire lifetime, (b) growing, (c) mature, and (d) decaying stages. Each bin contains a minimum of 10 samples. The bin-size is 0.02 for AOD < 0.5 and 0.2 for AOD > 0.5 (x axis). Mesoscale convective systems surrounded with AOD up to 1.5 are shown. Bins with the mean significantly different than the two standard errors of the samples (see section 2.2 and the supporting information) are only shown.

between 0.2 and 0.4 as VWS varies from a low value of $3.0 \times 10^{-4}/s$ to a moderate value of $21 \times 10^{-4}/s$ during the growing, mature, and decay stages (Figures 3b–3d), respectively. Throughout their entire lifetime (Figure 3a), TRVs from MCSs accumulate to volumes more than 10 km^3 or 80–170 mm at those optimal values of AOD and VWS compared to 2–4 km³ or 20–40 mm outside those optimal ranges. Thus, our

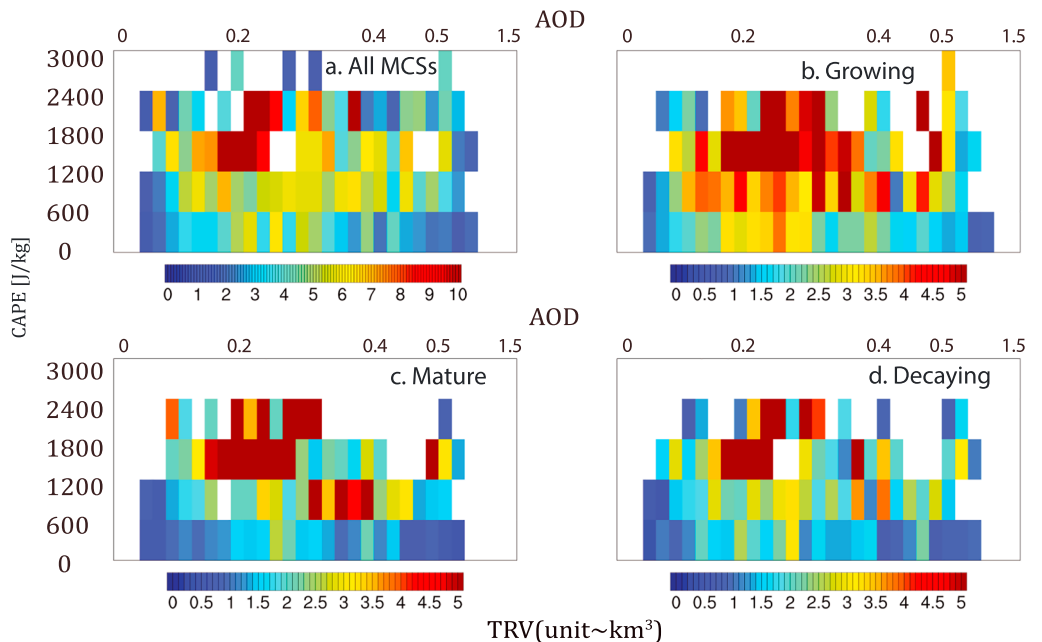


Figure 2. Same as in Figure 1 but total rain volume (TRV) as a function of aerosol optical depth (AOD) and convective available potential energy.

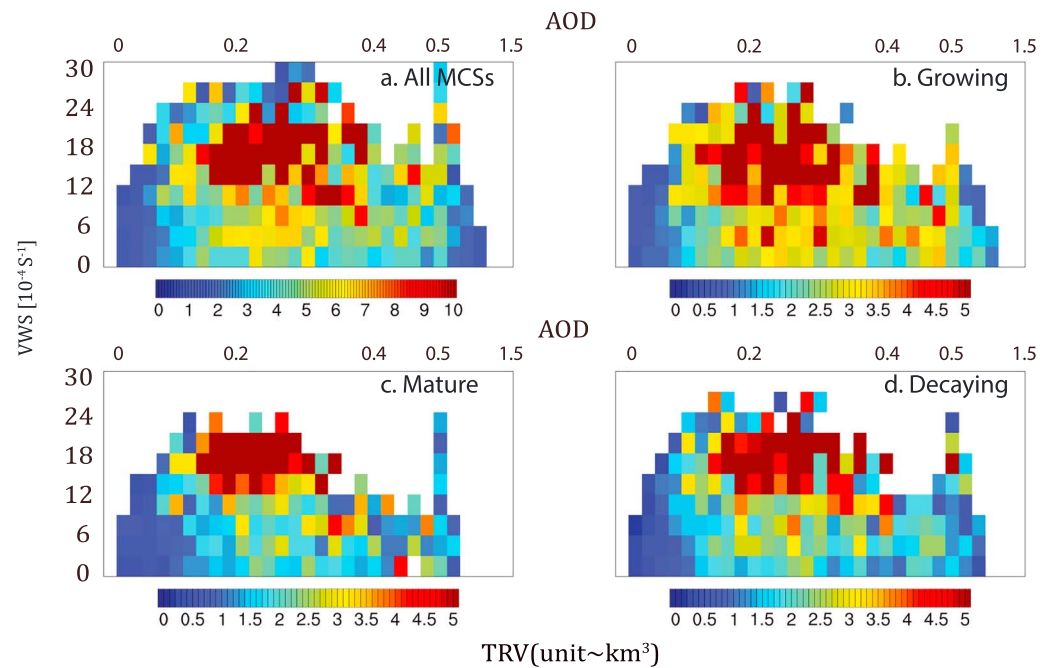


Figure 3. Same as in Figure 1 but TRV as a function of aerosol optical depth (AOD) and vertical wind shear.

analysis shows that the basic response of TRV to aerosol concentration is similar under all the meteorological conditions we considered and during all stages of the MCS lifecycle.

We also show similar patterns of variation of the TRV with respect to ambient relative humidity conditions (Figures S1 and S2) as those in Figures 1–3. TRV maximizes at moderate ranges of AOD between 0.2 and 0.4 when ambient RH is constant (Figures S1a–S1d and S2a–S2d). MCSs associated with RH_{850} greater than 80% generally have smaller size (maximum of mean radii of all MCSs ~ 170 km compared to 290–450 km for RH_{850} between 40 and 80%). These smaller MCSs contribute to lower TRV when RH is higher than 80% (Figures S1a–S1d). We also obtained similar patterns of the variation using TRMM 2A25 and MODIS AOD data sets (Figure S4). Since TRMM 2A25 data have a swath of 215 km, its data sometimes pertain to only a fraction of the larger MCSs. As a result, total TRV measured by using TRMM 2A25 data sets is less than that measured by using TRMM 3B42 data sets; however, TRV (Figure S4) also peaks when f_{AOD} (fraction of pixels with $AOD > 0.15$ to all the pixels surrounding a MCS (Chakraborty et al., 2016) ranges in between 30 and 70%.

4. Conclusions

Large MCSs that produce heavy rainfall are the primary cause of floods. Previous studies have hypothesized that aerosols can enhance rainfall and flood risk. However, whether aerosols can increase TRV throughout the entire lifetime of MCSs has not been clear in part due to the lack of adequate observations. The hypothesis that aerosols can invigorate deep convection and increase flood risk has been put forward by previous studies (Daniel Rosenfeld et al., 2008). Many studies have studied the influence of aerosols and meteorological conditions extensively. However, such potential impacts on the MCS either have been hypothesized or have been deduced based on campaign data sets. For example, Rosenfeld et al in 2008 hypothesized that the meteorological influence on the relationships between aerosols and MCSs' strength is nonlinear. As AOD increases, MCS's strength increases and after a threshold of 0.3, such effects on the MCSs reverse. This primarily occurs because of two major facts. First, the condensate loading effect reduces the buoyancy of the MCSs, delays precipitation (or condensate unloading), and makes the clouds heavy. Second is the AOD-radiation interactions. As AOD increases, the net radiation reaching the surface also reduces (Figure 4, Rosenfeld et al., 2008). This can reduce the surface warming, evaporation, and thus, the MCSs' strength. As a result of these combined microphysical and the radiation effects, MCSs weaken as AOD increases beyond 0.3. To

our knowledge, this work is the first to verify such effects observationally on a global tropical scale and identifies the optimal meteorological and aerosol conditions for such effects to occur based on a large number of samples (71,184) of MCSs over the global tropical continents. This study brings in the cloud lifecycle dimension into the analysis and we jointly consider aerosol and meteorology (CAPE, RH, TPW, and VWS) comprehensively in regard to the temporal, aerosol, dynamical, and variable scopes.

In particular, the TRV produced during the lifetime of the MCSs increases significantly with AOD when its value is below 0.4 for approximately fixed meteorological conditions. The increase of TRV with aerosols varies strongly with meteorological conditions and peaks at TPW (Figure 1) of 45–75 kg/m², CAPE (Figure 2) of 1200–2400 J/kg, or VWS (Figure 3) of 9–21 × 10⁻⁴/s. Within these ranges of the optimal meteorological conditions, the total TRV during the lifetime of the MCSs increases from 2 to 6 km³ when AOD < 0.15 to more than 10–12 km³ when 0.2 < AOD < 0.4 or from 20–40 mm to 80–170 mm (depending on the size of MCSs and meteorological conditions) of RD. In addition, our results suggest that the meteorological conditions, especially TWP, CAPE, and VWS, dominate the total variance of the TRV, explaining 54% and 62% of the total TRV variance during the growing and mature stages (Figures S8a and S8b), respectively. AOD has secondary influence, explaining 21% and 23% of the total TRV variance during the growing and mature stages, respectively. However, during the decay stage (Figure S8c), AOD explains 45% of the total TRV variance. Overall, AOD has a significant, although secondary, influence on TRV of the MCSs compared to that of the meteorological conditions at the global tropical continental scale. Our study confirms that TRV from MCSs increases as aerosol concentration increases with AOD up to 0.4. TRV starts decreasing as AOD increases further and becomes greater than 0.5. We have used a total of 71,184 samples at different stages of the convective lifecycles to prove that the basic response of TRV with aerosols is the same under all the meteorological conditions (TPW, RH, CAPE, and VWS) considered.

Although these results are empirical, they are generally consistent with the aerosol-cloud interaction processes reported in the literature (Holloway & Neelin, 2009; Houze, 2004; Weisman & Rotunno, 2004; Zipser, 1977). First, the increase of TRV with TPW, CAPE, and intermediate VWS is consistent with those reported in the literature and our general understanding of convective processes (Holloway & Neelin, 2009; Houze, 2004; Weisman & Rotunno, 2004). What processes might be responsible for the nonlinear behavior, that is, TRV increases with AOD from clean to moderately heavy pollution (AOD ranges from 0.0 to 0.4) and decreases under very heavy pollution (AOD > 0.5)? Previous studies (I. Koren et al., 2010; Daniel Rosenfeld et al., 2008) show that at moderate cloud condensation nuclei (CCN) concentrations, a parcel rising adiabatically can be more buoyant and can have a higher amount of released convective energy at the top of the cloud because of the released latent heat above the freezing level, an increased autoconversion rate, and a consequent unloading of the parcel by precipitation. At higher aerosol concentrations, the autoconversion rate slows down owing to a larger number of smaller CCNs; smaller cloud droplets reach the homogeneous nucleation level of –38 °C by updraft thrusts and freeze into smaller ice particles. Moreover, a reduction in the radiative energy reaching at the surface owing to a higher AOD can also reduce the convective vigor. These processes can weaken MCSs' precipitation and strength.

Chakraborty et al. (2016) have shown that AOD has a stronger influence on the total variance of the duration of the MCSs in the decay stage than does meteorological conditions, due to the increase of cloud ice in convective anvils with AOD. Similarly, AOD has the strongest influence on the total variance of TRV during the decay stage (Figure S8c) in part because of AOD increases both anvil cloud ice and the duration of the decay stage of the MCSs. Because the increase of TRV with aerosols appears to be very strong for MCSs that produce highest rainfall (Figures 1–3), aerosols tend to intensify extreme flood events, as hypothesized in the literature (Daniel Rosenfeld et al., 2008). This finding can be of particular relevance to regions prone to extreme rainfall and heavy pollution, such as South and East Asia. For example, rainfall over 200 mm was recorded in a major flood event that affected 20 million people in Pakistan in 2010 (Lankarani, 2010).

MCSs with AOD > 0.5 are expected to have longer lifetime because of the rain volume reduction with increasing AOD values; however, such relationships between rain volume and longevity for MCSs associated with AOD < 0.4 awaits additional studies. MCSs used in this analysis propagate to different locations with time, and their lifetime can be associated with their interactions with the environment, low-level convergence, and lateral entrainment of humidity, rather than the total rain volume only, for example, tropical cyclones or monsoon clouds.

This study does not provide information about the aerosol chemistry that plays an important role in cloud-aerosol microphysics. Further study using cloud microphysics including aerosol chemistry and CCN measurements using ground-based or aircraft measurements at the three different stages of the convective lifecycle is appropriate and needed to understand aerosol chemistry impacts on MCSs.

Acknowledgments

S. C. and R. F. were supported by the Office of Biological and Environmental Research within the Department of Energy (DOE), Office of Science, (DE-SC0011117). S. M. is supported by NASA CALIPSO/CLOUDSAT grant NNX14AO85G. We acknowledge the providers of the ISCCP, TRMM, MODIS, and MERRA data sets. All the analyzed data sets used for this study are publicly available for download, and links to such downloads are provided in section S1 in the supporting information.

References

- Bister, M., & Kulmala, M. (2011). Anthropogenic aerosols may have increased upper tropospheric humidity in the 20th century. *Atmospheric Chemistry and Physics*, 11(9), 4577–4586. <https://doi.org/10.5194/acp-11-4577-2011>
- Chakraborty, S., Fu, R., Massie, S. T., & Stephens, G. (2016). Relative influence of meteorological conditions and aerosols on the lifetime of mesoscale convective systems. *Proceedings of the National Academy of Sciences of the United States of America*, 113(27), 7426–7431. <https://doi.org/10.1073/pnas.1601935113>
- Cotton, W. R., & Anthes, R. A. (1989). *Storm and cloud dynamics*. San Diego, CA: Academic Press.
- de Boer, G., Hashino, T., & Tripoli, G. J. (2010). Ice nucleation through immersion freezing in mixed-phase stratiform clouds: Theory and numerical simulations. *Atmospheric Research*, 96(2–3), 315–324. <https://doi.org/10.1016/j.atmosres.2009.09.012>
- Fan, J. W., Leung, L. R., Rosenfeld, D., Chen, Q., Li, Z. Q., Zhang, J. Q., & Yan, H. R. (2013). Microphysical effects determine macrophysical response for aerosol impacts on deep convective clouds. *Proceedings of the National Academy of Sciences of the United States of America*, 110(48), E4581–E4590. <https://doi.org/10.1073/pnas.1316830110>
- Fan, J. W., Zhang, R. Y., Li, G. H., & Tao, W. K. (2007). Effects of aerosols and relative humidity on cumulus clouds. *Journal of Geophysical Research*, 112, D14204. <https://doi.org/10.1029/2006JD008136>
- Holloway, C. E., & Neelin, J. D. (2009). Moisture vertical structure, column water vapor, and tropical deep convection. *Journal of the Atmospheric Sciences*, 66(6), 1665–1683. <https://doi.org/10.1175/2008JAS2806.1>
- Houze, R. A. (2004). Mesoscale convective systems. *Reviews of Geophysics*, 42, RG4003. <https://doi.org/10.1029/2004RG000150>
- Houze, R. A., Rasmussen, K. L., Zuluaga, M. D., & Brodzik, S. R. (2015). The variable nature of convection in the tropics and subtropics: A legacy of 16 years of the Tropical Rainfall Measuring Mission satellite. *Reviews of Geophysics*, 53, 994–1021. <https://doi.org/10.1002/2015rg000488>
- Huffman, G. J., Adler, R. F., Bolvin, D. T., Gu, G. J., Nelkin, E. J., Bowman, K. P., & Stocker, E. F. (2007). The TRMM multisatellite precipitation analysis (TMPA): Quasi-global, multiyear, combined-sensor precipitation estimates at fine scales. *Journal of Hydrometeorology*, 8(1), 38–55. <https://doi.org/10.1175/Jhm560.1>
- Khain, A., Pokrovsky, A., Pinsky, M., Seifert, A., & Phillips, V. (2004). Simulation of effects of atmospheric aerosols on deep turbulent convective clouds using a spectral microphysics mixed-phase cumulus cloud model. Part I: Model description and possible applications. *Journal of the Atmospheric Sciences*, 61(24), 2963–2982. <https://doi.org/10.1175/Jas-3350.1>
- Khain, A., Rosenfeld, D., & Pokrovsky, A. (2005). Aerosol impact on the dynamics and microphysics of deep convective clouds. *Quarterly Journal of the Royal Meteorological Society*, 131(611), 2639–2663. <https://doi.org/10.1256/Qj.04.62>
- Khain, A. P., BenMoshe, N., & Pokrovsky, A. (2008). Factors determining the impact of aerosols on surface precipitation from clouds: An attempt at classification. *Journal of the Atmospheric Sciences*, 65(6), 1721–1748. <https://doi.org/10.1175/2007jas2515.1>
- Koren, I., Feingold, G., & Remer, L. A. (2010). The invigoration of deep convective clouds over the Atlantic: Aerosol effect, meteorology or retrieval artifact? *Atmospheric Chemistry and Physics*, 10(18), 8855–8872. <https://doi.org/10.5194/acp-10-8855-2010>
- Koren, I., Martins, J. V., Remer, L. A., & Afargan, H. (2008). Smoke invigoration versus inhibition of clouds over the Amazon. *Science*, 321(5891), 946–949. <https://doi.org/10.1126/science.1159185>
- Langhans, W., Yeo, K., & Romps, D. M. (2015). Lagrangian investigation of the precipitation efficiency of convective clouds. *Journal of the Atmospheric Sciences*, 72(3), 1045–1062. <https://doi.org/10.1175/Jas-D-14-0159.1>
- Lankarani, K. B. (2010). Pakistan floods. *Iranian Red Crescent Medical Journal*, 12(6), 606–607.
- Lee, S. S. (2012). Effect of aerosol on circulations and precipitation in deep convective clouds. *Journal of the Atmospheric Sciences*, 69(6), 1957–1974. <https://doi.org/10.1175/Jas-D-11-0111.1>
- Lee, S. S., Tao, W. K., & Jung, C. H. (2014). Aerosol effects on instability, circulations, clouds, and precipitation. *Advances in Meteorology*, 2014, 1–8. <https://doi.org/10.1155/2014/683950>
- Lin, J. C., Matsui, T., Pielke, R. A., & Kummerow, C. (2006). Effects of biomass-burning-derived aerosols on precipitation and clouds in the Amazon Basin: A satellite-based empirical study. *Journal of Geophysical Research*, 111, D19204. <https://doi.org/10.1029/2005JD006884>
- Machado, L. A. T., Rossow, W. B., Guedes, R. L., & Walker, A. W. (1998). Life cycle variations of mesoscale convective systems over the Americas. *Monthly Weather Review*, 126(6), 1630–1654. [https://doi.org/10.1175/1520-0493\(1998\)126<1630:Lcvomc>2.0.Co;2](https://doi.org/10.1175/1520-0493(1998)126<1630:Lcvomc>2.0.Co;2)
- Maddox, R. A., Chappell, C. F., & Hoxit, L. R. (1979). Synoptic and meso-alpha scale aspects of flash flood events. *Bulletin of the American Meteorological Society*, 60(2), 115–123. <https://doi.org/10.1175/1520-0477-60.2.115>
- Remer, L. A., Kaufman, Y. J., Tanre, D., Mattoo, S., Chu, D. A., Martins, J. V., et al. (2005). The MODIS aerosol algorithm, products, and validation. *Journal of the Atmospheric Sciences*, 62(4), 947–973. <https://doi.org/10.1175/Jas3385.1>
- Rienecker, M. M., Suarez, M. J., Gelaro, R., Todling, R., Bacmeister, J., Liu, E., et al. (2011). MERRA: NASA's Modern-Era Retrospective Analysis for Research and Applications. *Journal of Climate*, 24(14), 3624–3648. <https://doi.org/10.1175/Jcli-D-11-00015.1>
- Rosenfeld, D. (1999). TRMM observed first direct evidence of smoke from forest fires inhibiting rainfall. *Geophysical Research Letters*, 26(20), 3105–3108. <https://doi.org/10.1029/1999GL006066>
- Rosenfeld, D. (2000). Suppression of rain and snow by urban and industrial air pollution. *Science*, 287(5459), 1793–1796. <https://doi.org/10.1126/science.287.5459.1793>
- Rosenfeld, D., Fromm, M., Trentmann, J., Luderer, G., Andreae, M. O., & Servranckx, R. (2007). The Chisholm firestorm: Observed microstructure, precipitation and lightning activity of a pyro-cumulonimbus. *Atmospheric Chemistry and Physics*, 7(3), 645–659. <https://doi.org/10.5194/acp-7-645-2007>
- Rosenfeld, D., & Lensky, I. M. (1998). Satellite-based insights into precipitation formation processes in continental and maritime convective clouds. *Bulletin of the American Meteorological Society*, 79(11), 2457–2476. [https://doi.org/10.1175/1520-0477\(1998\)079<2457:Sbjipf>2.0.Co;2](https://doi.org/10.1175/1520-0477(1998)079<2457:Sbjipf>2.0.Co;2)
- Rosenfeld, D., Lohmann, U., Raga, G. B., O'Dowd, C. D., Kulmala, M., Fuzzi, S., et al. (2008). Flood or drought: How do aerosols affect precipitation? *Science*, 321(5894), 1309–1313. <https://doi.org/10.1126/science.1160606>

- Schumacher, C., Houze, R. A. Jr., & Kraucunas, I. (2004). The tropical dynamical response to latent heating estimates derived from the TRMM Precipitation Radar. *Journal of the Atmospheric Sciences*, *61*(12), 1341–1358. [https://doi.org/10.1175/1520-0469\(2004\)061<1341:TTDRTL>2.0.CO;2](https://doi.org/10.1175/1520-0469(2004)061<1341:TTDRTL>2.0.CO;2)
- Stevens, B., & Feingold, G. (2009). Untangling aerosol effects on clouds and precipitation in a buffered system. *Nature*, *461*(7264), 607–613. <https://doi.org/10.1038/nature08281>
- Tackett, J. L., & Di Girolamo, L. (2009). Enhanced aerosol backscatter adjacent to tropical trade wind clouds revealed by satellite-based lidar. *Geophysical Research Letters*, *36*, L14804. <https://doi.org/10.1029/2009GL039264>
- Tao, W. K., Chen, J. P., Li, Z. Q., Wang, C., & Zhang, C. D. (2012). Impact of aerosols on convective clouds and precipitation. *Reviews of Geophysics*, *50*, RG2001. <https://doi.org/10.1029/2011RG000369>
- Tulet, P., Crahan-Kaku, K., Leriche, M., Aouizerats, B., & Crumeyrolle, S. (2010). Mixing of dust aerosols into a mesoscale convective system generation, filtering and possible feedbacks on ice anvils. *Atmospheric Research*, *96*(2–3), 302–314. <https://doi.org/10.1016/j.atmosres.2009.09.011>
- van den Heever, S. C., Carrio, G. G., Cotton, W. R., DeMott, P. J., & Prenni, A. J. (2006). Impacts of nucleating aerosol on Florida storms. Part I: Mesoscale simulations. *Journal of the Atmospheric Sciences*, *63*(7), 1752–1775. <https://doi.org/10.1175/Jas3713.1>
- Van Den Heever, S. C., & Cotton, W. R. (2007). Urban aerosol impacts on downwind convective storms. *Journal of Applied Meteorology and Climatology*, *46*(6), 828–850. <https://doi.org/10.1175/Jam2492.1>
- Varnai, T., & Marshak, A. (2009). MODIS observations of enhanced clear sky reflectance near clouds. *Geophysical Research Letters*, *36*, L06807. <https://doi.org/10.1029/2008GL037089>
- Weisman, M. L., & Rotunno, R. (2004). “A theory for strong long-lived squall lines” revisited. *Journal of the Atmospheric Sciences*, *61*(4), 361–382. [https://doi.org/10.1175/1520-0469\(2004\)061<0361:Atfsls>2.0.Co;2](https://doi.org/10.1175/1520-0469(2004)061<0361:Atfsls>2.0.Co;2)
- Zhang, R. Y., Li, G. H., Fan, J. W., Wu, D. L., & Molina, M. J. (2007). Intensification of Pacific storm track linked to Asian pollution. *Proceedings of the National Academy of Sciences of the United States of America*, *104*(13), 5295–5299. <https://doi.org/10.1073/pnas.0700618104>
- Zipser, E. J. (1977). Mesoscale and convective-scale downdrafts as distinct components of squall-line structure. *Monthly Weather Review*, *105*(12), 1568–1589. [https://doi.org/10.1175/1520-0493\(1977\)105<1568:Macdad>2.0.Co;2](https://doi.org/10.1175/1520-0493(1977)105<1568:Macdad>2.0.Co;2)